Eur Biophys J (2012) 41:781–787
DOI 10.1007/s00249-012-0825-5

REVIEW

EBSA
Biophysics in Europe

Straight lines of neutron scattering in biology: a review of basic controls in SANS and EINS

Giuseppe Zaccai

Received: 24 February 2012 / Revised: 27 April 2012 / Accepted: 13 May 2012 / Published online: 30 May 2012

Abstract Neutron and X-ray beams in scattering experiments have similar wavelengths and explore the same length scale (~ 1 Å or 0.1 nm). Data collection and analysis are also broadly similar for both radiation types. There are fundamental differences, however, between the interaction of X-rays and neutrons with matter, which makes them strongly complementary for structural studies in biology. The property of neutrons to distinguish natural abundance hydrogen from its deuterium isotope and the dispersion relation that leads to the energy of ~ 1 Å neutrons being of the order of thermal energy are well known. They form the basis, respectively, of contrast variation on the one hand and energy-resolved scattering experiments to study macromolecular dynamics-neutron-specific scattering methods on the other. Interestingly, analysis procedures for the structural and dynamics experiments display common aspects that can be expressed as straight-line relationships. These not only act as controls of good sample preparation, but also yield model-free parameters on an absolute scale that provide fundamental information on the structure and dynamics of the system under study.

Keywords Small angle neutron scattering · Elastic incoherent neutron scattering · Elastic temperature scan · Macromolecular structure and interactions in solution · Macromolecular dynamics · Diffraction and scattering data analysis

Special Issue: Scattering techniques in biology—Marking the contributions to the field from Peter Laggner on the occasion of his 68th birthday.

The review is dedicated to Peter Laggner in gratitude for our many stimulating discussions on the science of life and life itself.

G. Zaccai (✉)
Institut Laue Langevin and CNRS, Grenoble, France
e-mail: zaccai@ill.fr

Introduction

In a diffraction experiment, waves of radiation scattered by an atomic arrangement in a sample interfere to give rise to an observable pattern, from which the structure of the sample could be deduced. The interference pattern arises when the wavelength of the radiation is similar to or smaller than the distances separating the objects. Atomic bond lengths are close to 1 Å unit (0.1 nm). X-ray and thermal neutron beams of wavelength ~ 1 Å are the most used probes to determine structure at the atomic and molecular levels. A useful radiation should also present appropriate properties of interaction with matter; it should not be absorbed too strongly and it should be scattered with reasonable efficiency. And, of course, radiation sources of appropriate intensity should be available. X-rays and neutrons broadly satisfy these criteria. There are significant differences in the details of their interaction with matter, however, that make them strongly complementary for diffraction studies of biological molecular structure. In this article, we discuss neutron scattering in the particular cases of small angle neutron scattering (SANS) to study (very) low-resolution structures and interactions of biological macromolecules in solution, and elastic incoherent neutron scattering (EINS) to study molecular dynamics.

Neutrons are scattered by atomic nuclei in a complex process. Because the neutron wavelength in diffraction experiments ($\lambda \sim 1$ Å, 10^{-10} m) is so much larger than nuclear dimensions ($\sim 10^{-15}$ m), nuclei act as points that scatter the wave isotropically, i.e., equally in all directions. Heavier elements do not dominate neutron scattering and

because the scattering is nuclear there is an isotope effect. The case of natural abundance hydrogen and deuterium (^{2}H or D) is of particular interest in structural biology. The neutron-scattering powers of H and D are sufficiently different from each other to provide useful labelling opportunities to observe hydrogen atoms and water molecules in biological samples.

The scattered neutron waves from a sample with a large number of atoms contain *coherent* and *incoherent* components. The *coherent* component is the result of interference between waves scattered by the atoms in their different locations in the sample; it contains structural information in SANS, neutron diffraction and crystallography experiments. The neutron-scattering power of a nucleus also depends on the relative orientation of nuclear and neutron beam spins. Neutron and nuclear spins can be polarised (oriented) by a magnetic field. However, unpolarised beams and samples are used in most diffraction experiments, so that the same type of nucleus in a sample will scatter neutrons with different powers according to the spin–spin orientations. The distribution of neutron-proton spin–spin orientations is random in the sample, resulting in a strong incoherent contribution to the scattering. Whereas the coherently scattered wave results from the sum of amplitudes of waves from all the atoms in the sample with their appropriate phase relationships, the incoherent wave results from the sum of the individual scattered intensities—the sum of single particle incoherent scattering. The effect is largest for the proton (the hydrogen nucleus) and results in hydrogen containing samples (H_2O solution for example) giving a high background signal in SANS, which does not contain structural information. The analysis of incoherent neutron scattering, however, provides information on sample molecular dynamics. It forms the basis of EINS experiments. The coherent scattering amplitudes and incoherent scattering cross sections of common atoms in biological molecules are given in Table 1.

Table 1 Coherent scattering amplitudes and incoherent scattering cross sections of common atoms in biological molecules

Nucleus	Coherent scattering length (10^{-12} cm)	Incoherent cross-section (10^{-24} cm^2)
H (natural abundance)	−0.374	80.26
^{2}H or D	0.667	2.05
C	0.665	~0
N	0.936	0.5
O	0.58	~0
P	0.513	~0
S	0.285	~0

http://www.ncnr.nist.gov/resources/n-lengths/

Small angle neutron scattering

In a standard SANS experiment to study macromolecular structures and interactions, the sample is a solution of ~mg/ml macromolecules in aqueous solvent containing appropriate buffer, salt, etc. The two initial assumptions for a straightforward analysis of the data are (Fig. 1):

1. The solution is monodisperse: all particles are identical.
2. There is no interparticle interference: particle positions and orientations are independent, and each particle scatters as if it were alone in the solution; scattered waves from atoms within the same particle interfere to give the final wave from the particle (sum amplitudes with appropriate phases). Waves from different particles do not interfere (sum intensities).

Importance of transmission

In contrast variation experiments (see, for example, Jacrot et al. 1977; Zaccai and Jacrot 1983; Johs et al. 2006; Laggner et al. 1981; Stuhrmann 2008), the water is H_2O, D_2O or a mixture of both. Because of the strong incoherent cross section of H (Table 1), solutions in H_2O will have much higher background scattering and a much higher attenuation of the direct beam (effective absorption) than solutions in D_2O.

$$T = \frac{I_{\text{Transmitted}}}{I_{\text{Incident}}} = \exp(-Sd)$$
$$\frac{1}{d}\ln T = -S \quad (1)$$

where T is the effective transmission of a sample of thickness d cm and S (cm^{-1}) is the total scattering of the

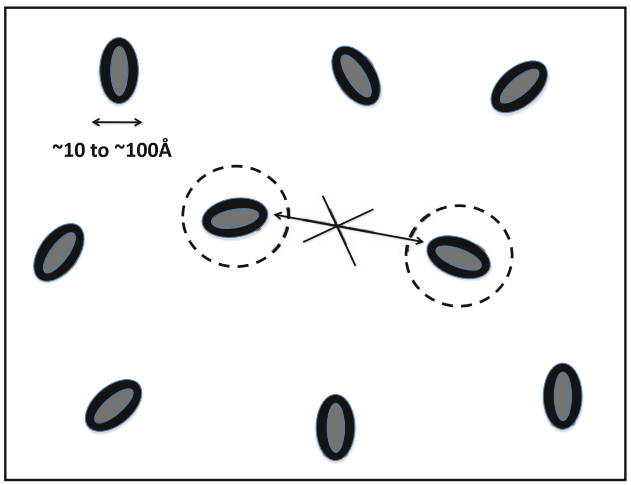

Fig. 1 'Ideal' solution scattering: particles are identical and take up random positions and orientations; waves scattered from within a particle interfere, not those scattered by different particles

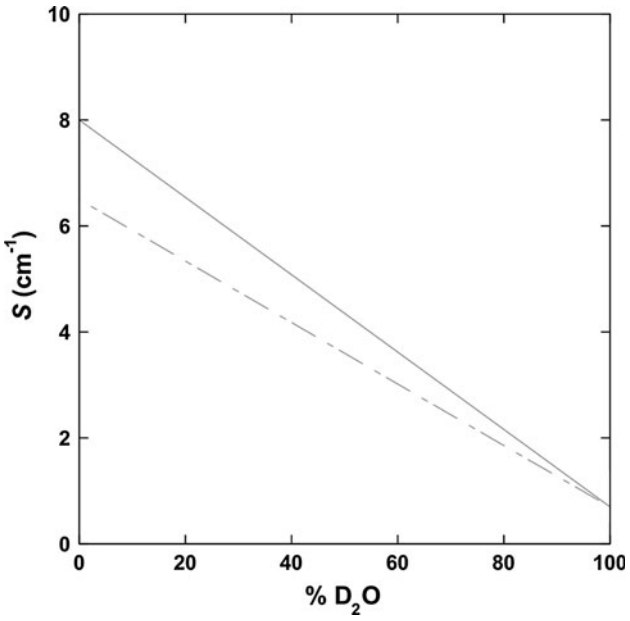

Fig. 2 Plot of $S = -(1/d)\ \ln T$ versus % D_2O in the sample (see text). The *full line* is for 6 Å, and the *dashed line* is for 10 Å wavelength neutrons, respectively

sample with contributions from the coherent and incoherent cross sections; the absorption cross section of these solutions is negligible. It is a very good approximation to write that S is simply linear with D_2O percentage in the sample solution—which gives us our first straight line for SANS (Fig. 2).

Sample scattering and therefore transmission are wavelength dependent. For example, the transmission of a 0.100 cm path length in H_2O is $\sim$0.45 for 10 Å and $\sim$0.52 for 6 Å wavelength neutrons. The corresponding values for 100 % D_2O are $\sim$0.93 for both wavelengths (incoherent scattering in D_2O is much weaker than in H_2O and the coherent scattering cross section contribution—which is not wavelength dependent—to the effective absorption is not negligible) (May et al. 1982). Clearly, 0.100 cm is a maximum path length for H_2O samples, and larger path lengths can be tolerated for D_2O samples. Transmissions of all samples should always be measured at the beginning of an SANS experiment, as a check on the wavelength setting and the D_2O % of the solutions. This is an important control to confirm that the buffer scatter subtraction is done correctly, i.e., that the D_2O % is the same for buffer and solution. As an example, consider 60 % D_2O (theoretically) sample and buffer preparations measured with a wavelength of 6 Å. The transmissions are measured, converted to $(1/d)\ \ln T$ and plotted on the dashed line in Fig. 2. T values of 0.70 and 0.73 for 0.100 cm paths of sample and buffer, respectively, indicate that the buffer was prepared correctly and corresponds to 60 % D_2O (-3.1 in the dashed line of Fig. 2); the sample value, on the other hand, falls on 3.5, indicating a D_2O % closer to 50 % (perhaps because of a dialysis that was not long enough). Buffer scatter, in this case, cannot be used for the background subtraction without appropriate correction. Note that, contrary to the SAXS case, in which background scattering increases strongly at small angles, buffer scattering in SANS is flat over the entire Q range (provided of course scattering is corrected for solid angle effects, when the detector is very close to the sample).

The Guinier approximation

The next step in a SANS experiment is to measure in the appropriate scattering vector modulus Q range ($Q = \frac{4\pi \sin\theta}{\lambda}$; 2θ is the scattering angle and λ is the wavelength) where the Guinier approximation is valid; i.e., in a Q range $\sim(1/R_G)$, where R_G is the expected radius of gyration value, which defines the length scale of the particle. In mechanics, the radius of gyration depends on the distribution of mass around the centre of mass. In a scattering experiment, the R_G is the distribution of excess scattering length or contrast, ($\left(\sum_m b - \rho^0 V_m\right)$ see below). The Guinier approximation is written:

$$\ln I(Q) = \ln I(0) - \frac{1}{3} R_G^2 Q^2 \tag{2}$$

If the sample is not aggregated, the Guinier plot provides our second straight line from which two model free experimental parameters are calculated: the forward scattering intensity, $I(0)$ (calibrated with respect to the direct beam intensity), and the radius of gyration (from the slope). The molar mass of the particle is calculated from $I(0)/c$ (c is concentration) and the composition of the particle (Jacrot and Zaccai 1981).

$$\frac{I(0)}{cTd} = \text{const.} \times N_A \left(\frac{\sum_m b - \rho^0 V_m}{m}\right)^2 M \tag{3}$$

The constant is instrument dependent to put the scattering on an absolute scale, c is concentration in g/ml, $\sum_m b$ and V_m are the sum of scattering amplitudes and volume in a relative molar mass m of the particle, and ρ^0 is the scattering length density of the solvent, so that the term in the brackets is the effective scattering amplitude (including contrast) per unit mass of particle; M is the molar mass of the particle in the solution. Each side of equation (3) is in units of cm^2/g. Scattering density calculations and other useful SANS information can be found at http://www.ncnr.nist.gov/resources/.

The Guinier parameters are important absolute scale controls from which the length scale and mass of the scattering particle are calculated, before modelling approaches are applied to the scattering curve at larger angles [e.g. see Chap. G2 in (Serdyuk et al. 2007)].

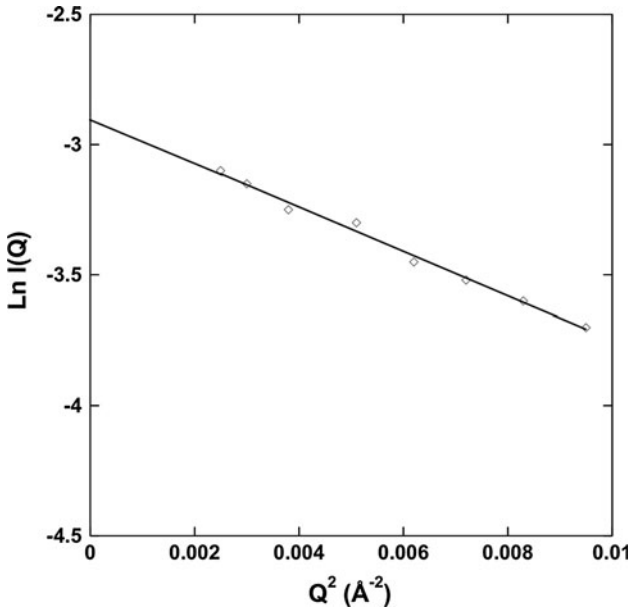

Fig. 3 Guinier plot for the membrane protein bacteriorhodopsin reconstituted into deuterated DMPC lipid vesicles in solvent % D_2O that contrast matches the lipid scattering. Redrawn from (Hunt et al. 1997)

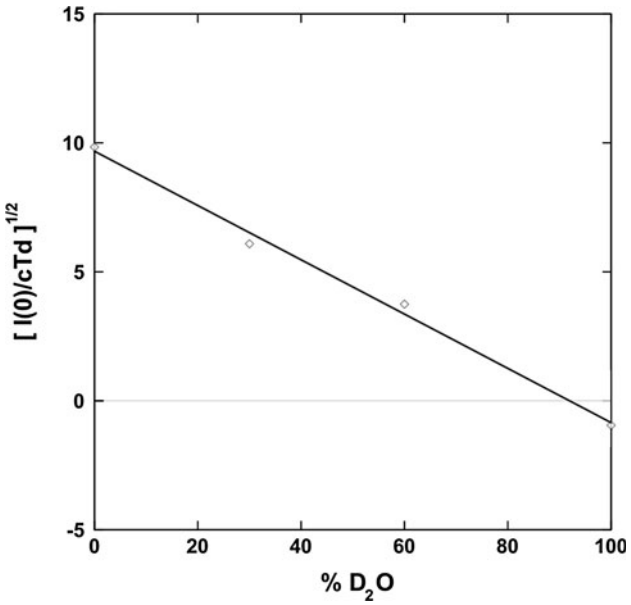

Fig. 4 Also from (Hunt et al. 1997), the contrast variation plot of deuterated lipid vesicles in various % D_2O solutions. The contrast match point is close to 90 % D_2O

An example of a Guinier approximation plot from (Hunt et al. 1997) is shown in Fig. 3.

In a contrast variation series, the $I(0)$ value is used to check for monodispersity in all % D_2O conditions corresponding to the same particle and to determine the contrast match point. Equation (3) shows that $\sqrt{\frac{I(0)}{cTd}}$ is linear with % D_2O (b is linear with % D_2O because of exchange of labile hydrogen in the particle, and ρ^0 is of course linear with % D_2O). This gives us our third straight line.

D_2O unfortunately favours aggregation, so that the straight line in Fig. 4 is an important control that the solution remains monodisperse. Note that if the solution properties change in any way (other than through contrast due to the % D_2O in the solvent) the points will not fall on a straight line.

Pitfalls of contrast variation

Aggregation due to D_2O effects is only one of the pitfalls to be avoided in contrast variation. In a contrast variation experiment of a two-component system (e.g. a protein–nucleic acid complex or a membrane protein in a lipid vesicle), the aim is to 'mask' out one of the components at the appropriate % D_2O in order to observe the other. A necessary condition for this to happen is that the component to be matched should be homogeneous in scattering density. Clearly, if this were not so, the mean scattering density would be matched by the %D_2O ($I(0) = 0$); however, areas of higher and lower scattering density would still contribute significantly to $I(Q)$, at $Q \neq 0$. How 'homogeneous' should the component be? This depends on the length resolution required. Simply put, the component to be matched should be homogeneous on the length scale of the component that is to be observed. The point is illustrated in Fig. 5 for protein–nucleic acid complexes. A protein is not homogeneous in scattering density because the scattering length densities are different for the different amino acid residues and because of exchangeable 'labile' H atoms [see Table in (Jacrot 1976)]. Like the elliptical particles drawn in Fig. 5, a soluble protein could be seen as having a denser scattering density outer shell, where hydrophilic amino acid residues dominate and a less dense core dominated by hydrophobic amino acids. The dashed double arrows in Fig. 5 represent the length scale of the inhomogeneity. Nucleic acid, by its chemical composition and structure, is quite homogeneous in scattering density. In Fig. 5, nucleic acid is represented by grey arcs and the corresponding length scales by bold double arrows. The protein will appear as homogeneous on the length sale of the nucleic acid for the complex in (A), but not for the complex in (B). The (A) case is similar to the case of the ribosome (Ramakrishnan 1986). The (B) case is similar to that of an aminoacyl-tRNA-synthetase complex with tRNA study, in which it was possible to match out the tRNA to study protein conformational changes upon binding, but not to match out the protein (Dessen et al. 1978).

The case of a membrane protein in a lipid vesicle is illustrated in Fig. 6. In their study of bacteriorhodopsin reconstituted in a lipid vesicle (Hunt et al. 1997) had to use deuterated lipids. Because of the scattering density

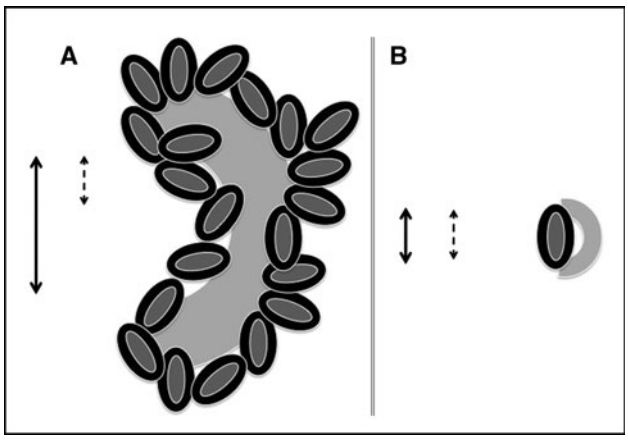

Fig. 5 Contrast variation of protein–nucleic acid complexes. The *dashed double arrows* represent the length scale of the protein inhomogeneity (denser, *black* hydrophilic shell). The *grey arc* is nucleic acid; its length scale is represented by the *bold double arrow*. **a** A large nucleic acid component. **b** A nucleic acid component of similar size to the protein

difference between the natural abundance lipid headgroups and fatty acid chains (Fig. 6a), it would have been impossible to match out the lipid in order to observe the protein alone, as was the aim of the experiment.

Neutron scattering density inhomogeneity is mainly due to H atom content. It is important to note that, in general, deuteration will reduce scattering density inhomogeneity. Using deuterated protein components is essential to match out parts of a protein–protein complex, as was performed by King et al. (2005) in their study of troponin. Deuteration will also make a protein more homogeneous in scattering density so that it can be matched out in a protein–nucleic acid complex to study nucleic acid conformational changes, in cases where protein and nucleic acid are on similar length scales.

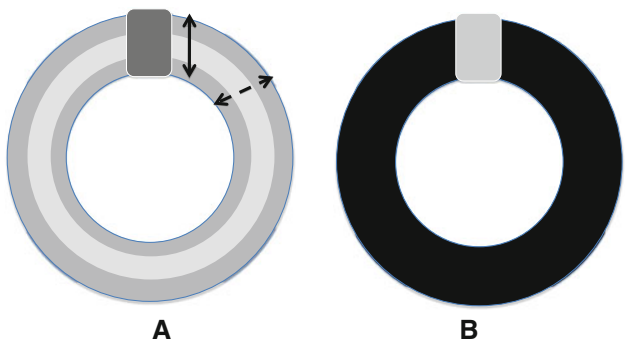

Fig. 6 Schematic diagram of a membrane protein (*grey rectangle*) in a lipid vesicle (*doughnut shape*). The *bold double arrow* is the length scale of the protein. The *dashed double arrow* is the length scale of the headgroup separation. **a** Natural abundance lipid, where the difference in scattering density between headgroup and hydrocarbon chains is significant. **b** The vesicle is closer to homogeneous in scattering density when the lipid is deuterated

The hydration shell of biological macromolecules constitutes another dangerous pitfall for contrast variation studies in SANS. The hydration shell is a volume of 'solvent' surrounding the macromolecule of different composition and/or structure than the bulk solvent in the solution (typically of ~10 % difference in density). In proteins, it extends for a molecular layer or two of water, while in nucleic acids (which are polyelectrolytes) depending on salt conditions it could extend much further from the macromolecular surface. Because of the hydration shell contribution, the contrast radius of gyration of tRNA in D_2O solution, for example, was found to be significantly smaller than in H_2O, for an identical macromolecular conformation (Li et al. 1983). In general, the contribution of hydration shell scattering will depend on contrast and resolution conditions. In H_2O, the solvent scattering density is very low and the hydration shell contribution will be negligible. In D_2O solution, however, it could be dominant, as revealed in the tRNA example.

Elastic incoherent neutron scattering

The energy and momentum changes measured in a neutron spectroscopy experiment are related to the time scales and amplitudes of atomic motions, respectively. In the incoherent scattering process, only neutron waves scattered by the *same* nucleus interfere to provide information on how the nucleus moves (Gabel et al. 2002). The incoherent cross section of natural abundance H is much larger than that of other nuclei, including that of the deuterium isotope (Table 1). This provides opportunities to label different components of a complex system in order to modulate their respective scattering contributions (Gabel et al. 2002). The most efficient and arguably most useful neutron spectroscopy method to measure dynamics is the *Elastic Temperature Scan*, in which the momentum change of elastically scattered neutrons is measured for different temperatures (Zaccai 2011a). A simple analysis provides the mean square displacements (MSD) of atomic motions as a function of temperature, as they are 'seen' with the energy resolution (time scale) and scattering vector, Q, range (length scale) of the spectrometer. The experimental MSDs are on an absolute scale ($Å^2$), and an effective force constant for the motions (*resilience*, $\langle k' \rangle$) also on an absolute scale (N/m) is calculated from the temperature dependence (Zaccai 2000). Qualitatively, the MSD will rise more steeply with temperature for a softer (less resilient) sample (on the atomic scale). The time scale depends on the neutron spectrometer used and varies between ~picosecond and ~nanosecond (Zaccai 2011a). This is very useful as it includes the time scales of protein internal thermal motions and the usual time range of molecular dynamics calculations (Kneller 2005).

An analysis similar to the Guinier approximation

In Fig. 1, the grey ellipsoids represent particles in solution. Waves scattered by atoms within a particle interfere, but not waves scattered by atoms in different particles. Figure 7 appears to be identical to Fig. 1, except for the length scale bar that is now ~Å.

EINS is scattering by a nucleus undergoing localised motion, i.e. moving well within the length–time window defined, respectively, by the Q range and energy resolution of the neutron spectrometer (Zaccai 2011a). Typical length–time windows to observe internal motions in a macromolecule are of the order of a few Å in 0.1–1 ns. The influence of Q range and energy resolution on the measurement of EINS has been analysed by Gabel (2005). H atoms dominate incoherent scattering (Table 1). Well localised in this window, H atoms in amino acid residues in a protein, for example, move with the groups to which they are bound and reflect macromolecular internal motions well. The particles in Fig. 7 could, therefore, represent H atoms in a macromolecule. By analogy with the Guinier approximation (from a comparison of Figs. 1, 7), the MSDs, $\langle u^2 \rangle$, of the motions are related to the radius of gyration of the motion and can be calculated from a Gaussian approximation (Réat et al. 1997).

$$\ln I(Q) = \ln I(0) - \frac{1}{6}\langle u^2 \rangle Q^2 \tag{4}$$

where (comparing with Eq. 2) $\langle u^2 \rangle = 2R_G^2$. Equation (4) is our first straight line for EINS (Fig. 8).

The mean energy $\langle E \rangle$ of a linear simple harmonic oscillator is related to the MSD by a force constant $\langle k' \rangle$.

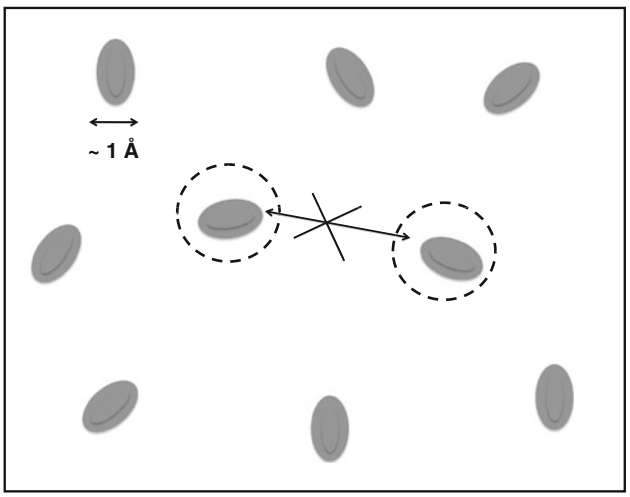

Fig. 7 Incoherent scattering by moving single hydrogen atoms in a macromolecular structure. Each atom traces an ellipsoidal volume well contained in the length–time window of the experiment. Waves scattered by the same atom as it takes up different positions in time within the ellipsoid interfere with each other. Waves from atoms particles do not interfere

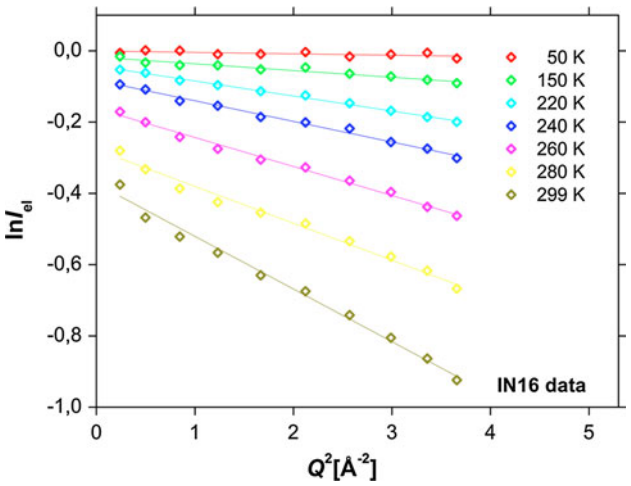

Fig. 8 Atomic scale dynamics of heparan sulphate on the nanosecond time scale. EINS intensity plotted in the Gaussian approximation (Eq. 4) at different temperatures with corresponding linear fits. Data were collected on the IN16 spectrometer (http://www.ill.eu/instruments-support/instruments-groups/instruments/in16/). From Jasnin et al. (2010)

$$\langle E \rangle = \frac{1}{2}\langle k \rangle \langle u^2 \rangle \tag{5}$$

The energy associated with the MSD of molecular dynamics is proportional to absolute temperature by Boltzmann's constant, $k_B T$. If the MSD is linear with T (the second straight line of EINS, Fig. 9) then, in a quasi-harmonic approximation, Eq. (5) can be re-written as

$$\langle u^2 \rangle = \frac{2}{\langle k' \rangle} k_B T \tag{6}$$

where $\langle k' \rangle$ is now an effective force constant that was named *resilience* (Zaccai 2000).

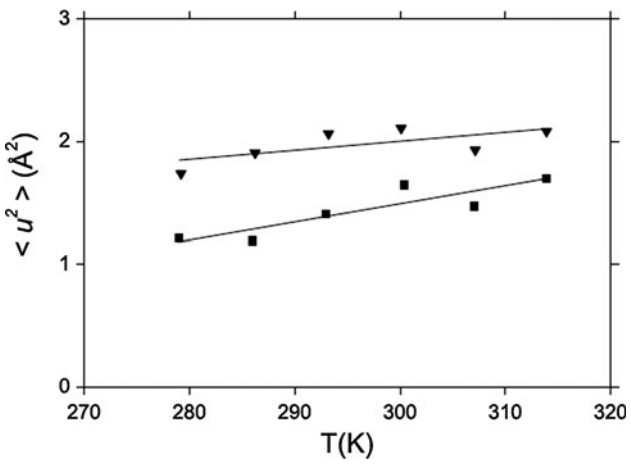

Fig. 9 Water isotope effect on molecular dynamics in live cells. MSD versus absolute temperature for internal macromolecular motions in *E. coli* cells in H_2O (*bold triangles*) and in D_2O (*bold squares*). Corresponding resilience values are 0.38 and 0.19 N/m, respectively. From Jasnin (2009)

In the example shown in Fig. 9, macromolecular motions in *E. coli* cells have a larger MSD in H_2O than in D_2O, but the resilience is lower in D_2O (0.17 N/m compared to 0.38 N/m) (Jasnin et al. 2008). Since D_2O stabilises macromolecular structures, the lower resilience was interpreted as an entropic factor favourable to stability, arising from higher degree of conformational sampling, itself related to a stronger hydrophobic effect in D_2O.

As illustrated by the water isotope effect, protein dynamics are more sensitive to the environment than structure. The ecology of protein dynamics was reviewed by Zaccai (2011b). At low temperatures (below about 200 K or −70 °C) protein internal motions behave as harmonic solids with low MSD and $\langle k' \rangle$ values between 1 and 4 N/m, measured for hydrated powder samples of haemoglobin, myoglobin and ribonuclease. At physiological temperatures, the resilience values are ten times lower in the same hydrated powder samples, and even lower when the protein is in solution. Haemoglobin resilience, for example, is 3 N/m at low temperature; at physiological temperature, it falls to 0.3 N/m with MSD of 1.0 $Å^2$ when the protein is in a D_2O-hydrated powder, and 0.17 N/m with MSD of 1.6 $Å^2$ for the protein measured in situ in red blood cells. The ecology of protein dynamics review (Zaccai 2011b) also deals with adaptation to extreme environments through dynamics and other dynamics-function relations in various soluble and membrane proteins, nucleic acids, lipids and cell surface polysaccharides.

Summary

A set of linear relations for data collected in SANS (to measure low resolution structures and interactions in solution) and elastic incoherent neutron scattering (to measure molecular dynamics) act as important controls for the validity of the experiments and provide fundamental, essentially model-free information on the system studied.

Acknowledgments I am grateful to Frank Gabel for a critical reading of the manuscript.

References

Dessen P, Blanquet S, Zaccai G, Jacrot B (1978) Antico-operative binding of initiator transfer RNAMet to methionyl-transfer RNA synthetase from *Escherichia coli*: neutron scattering studies. J Mol Biol 126:293–313

Gabel F (2005) Protein dynamics in solution and powder measured by incoherent elastic neutron scattering: the influence of Q-range and energy resolution. Eur Biophys J 34:1–12

Gabel F, Bicout D, Lehnert U, Tehei M, Weik M, Zaccai G (2002) Protein dynamics studied by neutron scattering. Q Rev Biophys 35:327–367

Hunt JF, McCrea PD, Zaccai G, Engelman DM (1997) Assessment of the aggregation state of integral membrane proteins in reconstituted phospholipid vesicles using small angle neutron scattering. J Mol Biol 273:1004–1019

Jacrot B (1976) The study of biological structures by neutron scattering from solution. Rep Prog Phys 39:911–953

Jacrot B, Zaccai G (1981) Determination of molecular weight by neutron scattering. Biopolymers 20:2413–2426

Jacrot B, Chauvin C, Witz J (1977) Comparative neutron small-angle scattering study of small spherical RNA viruses. Nature 266: 417–421

Jasnin M (2009) Intracellular dynamics in *E. coli* studied by incoherent neutron scattering and isotope labelling physics, vol PhD. Joseph Fourier University, Grenoble

Jasnin M, Tehei M, Moulin M, Haertlein M, Zaccai G (2008) Solvent isotope effect on macromolecular dynamics in *E. coli*. Eur Biophys J 37:613–617

Jasnin M, van Eijck L, Koza MM, Peters J, Laguri C, Lortat-Jacob H, Zaccai G (2010) Dynamics of heparan sulfate explored by neutron scattering. Phys Chem Chem Phys 12:3360–3362

Johs A, Hammel M, Waldner I, May RP, Laggner P, Prassl R (2006) Modular structure of solubilized human apolipoprotein B-100. Low resolution model revealed by small angle neutron scattering. J Biol Chem 281:19732–19739

King WA, Stone DB, Timmins PA, Narayanan T, von Brasch AA, Mendelson RA, Curmi PM (2005) Solution structure of the chicken skeletal muscle troponin complex via small-angle neutron and X-ray scattering. J Mol Biol 345:797–815

Kneller GR (2005) Quasielastic neutron scattering and relaxation processes in proteins: analytical and simulation-based models. Phys Chem Chem Phys 7:2641–2655

Laggner P, Kostner GM, Rakusch U, Worcester D (1981) Neutron small angle scattering on selectively deuterated human plasma low density lipoproteins. The location of polar phospholipid headgroups. J Biol Chem 256:11832–11839

Li ZQ, Giege R, Jacrot B, Oberthur R, Thierry JC, Zaccai G (1983) Structure of phenylalanine-accepting transfer ribonucleic acid and of its environment in aqueous solvents with different salts. Biochemistry 22:4380–4388

May RP, Ibel K, Haas J (1982) The forward scattering of cold neutrons by mixtures of light and heavy water. J Appl Crystallogr 15:15–19

Ramakrishnan V (1986) Distribution of RNA and protein in the 30S ribosomal subunit. Science 231:1562–1564

Réat V, Zaccai G, Ferrand M, Pfister C (1997) Functional dynamics in purple membranes. In: Cusack S, Büttner H, Ferrand M, Langan P, Timmins P (eds) Biological macromolecular dynamics. Adenine Press, Schenectady, pp 117–122

Serdyuk IN, Zaccai N, Zaccai G (2007) Methods in molecular biophysics: structure, dynamics, function. Cambridge University Press, Cambridge

Stuhrmann HB (2008) Small-angle scattering and its interplay with crystallography, contrast variation in SAXS and SANS. Acta Crystallogr A 64:181–191

Zaccai G (2000) How soft is a protein? A protein dynamics force constant measured by neutron scattering. Science 288:1604–1607

Zaccai G (2011a) Neutron scattering perspectives for protein dynamics. J Non Cryst Solids 357:615–621

Zaccai G (2011b) The ecology of protein dynamics. In: Jalkanen KJ (ed) Current Physical Chemistry, special issue on Quantum Nanobiology and Biophysical Chemistry (in press)

Zaccai G, Jacrot B (1983) Small angle neutron scattering. Annu Rev Biophys Bioeng 12:139–157